Membrane Technology
ISSN (online): 1873-4049

Analysis of Resistance Reduction via Support Vector Regression and Experiment on a Submerged Floating Vehicle Fitted with an Air Curtain Traversing Deep Soft Terrains

Chuan Huang[1], Shichun Yang[1], Wen Zeng[2,*], Guoyan Xu[1], Jian Wang[1], Feng Gao[1]

[1]School of Transportation Science and Engineering, Beihang University, Beijing 100191, China
[2]School of Automotive Engineering, Changzhou Institute of Technology, Changzhou 213032, China
**Corresponding Author.*

Abstract:
To improve the driving efficiency of submerged floating vehicles (SFVs) in deep soft terrains, the effect of an active air curtain method on the reduction and optimization of sliding resistance of a floating device was explored. The sliding resistance reduction principle of the air curtain was introduced, then, the resistance was analyzed. The soil bin experiment for air curtain resistance reduction test was built. The orthogonal tests were employed to ascertain the influence of the air curtain, ground contact pressure, sliding velocity, and soil moisture content upon the sliding resistance. The results show that the resistance with air curtain is less than that without air curtain, and the resistance reduction rate up to 11.17%. The resistance augments in tandem with the elevation of the ground contact pressure and the sliding velocity. When the soil moisture content approximates the liquid limit, the rate of resistance reduction reaches its peak. Furthermore, a support vector regression (SVR) method is put forward to formulate a regression prediction model for the sliding resistance. The predictions yielded by this method were proximate to the experimental outcomes. It implies that the SVR model exhibits a superior prediction capacity even with a restricted number of samples. The research discloses the impact of the air curtain, ground contact pressure, the floating device's sliding velocity, and soil moisture level on the sliding resistance. It lays a solid research foundation for the drag reduction design of submerged floating vehicles in deep soft terrains.

Keywords: air curtain, floating device, deep soft soils, sliding resistance, support vector machine, machine learning.

INTRODUCTION

Submerged Floating Vehicle

Deep mud paddy field is a typical terrain of deep soft clay. Its characteristic is high moisture content, which will reduce the bearing capacity of the soil. It is strongly required that a special walking mechanism is developed to adapt the deep soft clay. A submerged floating vehicles is the special walking mechanism, which slides on deep soft terrain with the floating device and moves by driving wheels [1]. It is evident that the ground contact area could be enlarged by the floating device of the submerged floating vehicle. The floating device can fully utilize the thrust and decrease the moving resistance produced by the soil.

As shown in Figure 1(a), the boat-shaped paddy tractor is a typical submerged floating vehicle [2]. Yao Xiaojiang developed a multi-terrain mobile platform, which was also a submerged floating vehicle, with the new traction mechanisms (variable diameter wheels) [3]. Liu Jie designed a wheel with slip-boots (as depicted in Figure 1(b)), which was implemented in the multi-terrain mobile platform, with the aim of enhancing the trafficability of the traction mechanism [4, 5].

(a) A boat-shaped paddy tractor (b) A multi-terrain mobile platform

Figure 1. Two typical submerged floating vehicles

Owing to the larger ground contact area of the floating device, the ground pressure on the front part of the traction mechanism can be diminished. The boat-shaped paddy tractor is propelled by the wheels with blades. Meanwhile, the boat-shaped device

slides on the soil [6]. When the traction device travels across deep soft clay, its resistance is significantly less than that of the wheel.

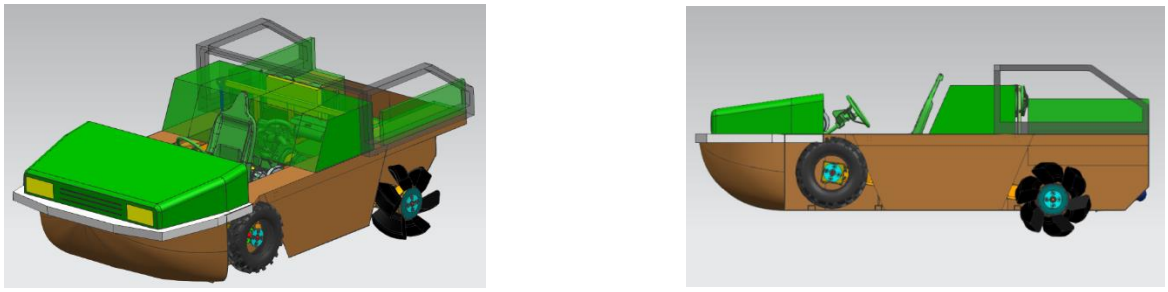

(a) An all-terrain vehicle (b) All-terrain vehicle on deep soft terrains

Figure 2. Amphibious all-terrain vehicle

An all-terrain vehicle, which is equipped with transformable back wheels, has been developed (as shown in Figure 2) [1]. The vehicle is capable of traversing deep soft clay and traveling on highway by adjusting the chassis posture. In the case of deep soft ground, the front wheels are folded up while the rear wheels are converted into walking wheels [as depicted in Figure 2(b)]. Hence, the vehicle is a submerged floating vehicle. When all wheels are laid down and the back wheels are folded into the circular wheels, the vehicle is able to travel on highway in a manner similar to that of a traditional vehicle.

The floating device of a submerged floating vehicle is the passive walking mechanism, which supports the vehicle body. The floating device slides on deep soft terrains while the submerged floating vehicle travels. Research on sliding walking mode mainly concentrates on the interaction happened on contact surfaces and travel characteristic of the sliding device. Sliding resistance of the floating device between undersurface and clay is an important evaluation parameter for the travel characteristic of the submerged floating vehicle.

Resistance Reducing by Air Curtain

The approaches for resolving the adhesion issues of the soil-contacting parts of terrain machinery can be approximately classified into five categories: enhancing the desorption conditions of soil adhesion between interfaces, mechanical processing, shape alteration, surface modification and biomimetic approach. These methods are active or passive [7]. The main idea of active methods makes soil not to adhere on the surface of soil touching parts of terrain machinery. However, the passive methods take away soil that have been adhered on the surface of the soil touching parts. It is worth pointing out that the sliding resistance reduction by air curtain is an active method [7].

Many researchers concentrate on the resistance reduction via air curtain for the field of vessels navigating in water [8-14]. Currently, there are two typical explanations about resistance reduction by air curtain. McCormick and Bhattacharyya proposed that the area of high shearing force closed to the wall was eliminated while the bubble collapsing at the adhesion layer [15]. Madavan and other prominent scholars suggested that resistance could be reduced due to the change of stickiness and density [16]. Submerged floating vehicles travelling on deep soft clay are different from vessels navigating in water, but there are also similarities. The similarity is the mechanism of contacting with water because there is macroscopical water on the surface layer of the deep soft clay with high moisture content. The difference is the solid medium of soil particles. When a submerged floating vehicle travels on terrain, the shape of terrain and the distribution of ground pressure will be changed. It will result in increase of driving resistance and reactive resistance.

Over the years the method of reducing soil adhesion by air curtain has been used in some working equipment such as excavator, carry-scraper, bulldozer, plough and so on [7]. According to the theory of adhesion resistance reducing by air curtain, the compressed air is pumped into the space that between the soil touching parts of terrain machinery and deep soft clay through the air vent on the terrain machinery. Discontinuous air curtain floor will be build and the adhesion friction state will be altered partly to achieve the objective of reducing resistance [17].

Machine Learning

The air curtain, sliding velocity, ground contact pressure, and soil moisture level all exert an influence on the sliding resistance of the SFV. Owing to the multi-factor nature on deep soft terrain, the difficulty resides in predicting the sliding resistance. It is desirable to explore a novel approach to analyze the sliding resistance. Machine learning techniques are appropriate for extracting meaningful features from complex conditions, which are applied to object classification, prediction, and decision-making [18-

20]. Machine learning has been widely used, such as cancer detection, medical imaging [21], computer vision and voice recognition and face recognition [22]. Thus, it is believed that machine learning can establish algorithms and models that is able to learn to predict from the experiments of the sliding resistance.

Objective

The paper will explore the sliding resistance and investigate the mechanism of reducing the resistance by means of an air curtain with reference to the all-terrain vehicle. It is structured as follows: the mechanism of reducing the sliding resistance by the air curtain for the floating device is analyzed in Section 2. Section 3 outlines the experimental principle and the operational way. The orthogonal experiments and the analysis of the results is presented in Section 4. The SVR model to fit and predict the sliding resistance is constructed in Section 5. Section 6 provides a summary.

MECHANISM OF RESISTANCE REDUCTION BY AIR CURTAIN

Sliding Resistance

A floating device is simplified into the sliding plate. Its mechanics characteristics includes vertical load W loaded by the body of vehicle and moving resistance F. The moving resistance F consists of sliding resistance FS, bulldozing resistances T1,T2, and soil compacting resistance Fq, as shown in Figure 3. The sliding resistance is comprehensive embodiment of friction, adsorption, pushing and pulling. The friction and adsorption are the major. From a microscopic perspective, the primary influence on the sliding performance lies in the interaction among solid, liquid, or gas within the objects.

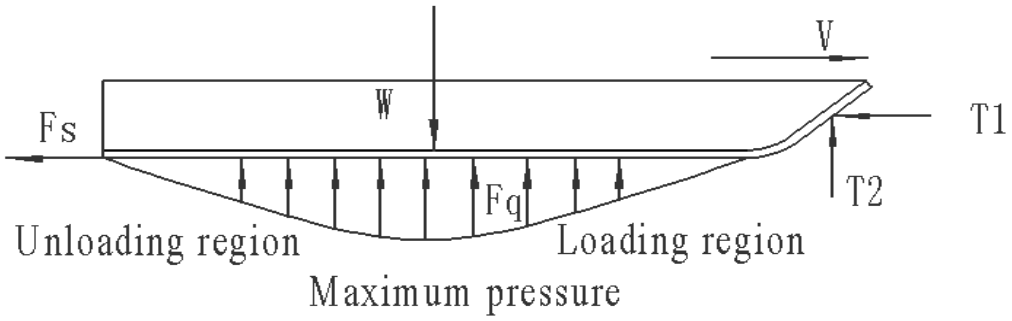

Figure 3. Sliding plate on soft terrain

Water or air film existing between the contacting bodies is the most important impact on the superiority of the sliding behavior. The sliding plate will sink into soft soil subjected to dead weight due to the low bearing capacity of deep soft clay. The sludge will overflow from the body on both sides under such compaction that will make the bottom of the floating device contact with the soil directly. Friction resistance will occur on the floating device as a result of the relative movement on the soft soil. The resistance follows the Coulomb principle, as shown in formula (1) [23].

$$F_s = cA + P\tan\varphi \tag{1}$$

Where c represents soil cohesion, φ represents internal friction angle of soft soil, A is contact area between the bottom of floating device and the soil, P is normal pressure on the bottom of floating device pressed by the soil. Formula (1) shows that the sliding resistance increases with the increase of the contact area. The principal approach to diminishing the frictional resistance is to reduce the contact area.

Breakaway Resistance and Steady Resistance

The sliding resistance can be classified into breakaway resistance and steady resistance. Free water on the surface of soil will be extruded by the floating device, which will increase the sliding resistance and aggravate the soil adhesion. Especially, it is more difficulty while the mechanism launching. This is due to the increase of contact area between the floating device and the soil. Breakaway resistance will increase because of the increase of adhesion. The breakaway resistance can be defined as the maximum resistance during the starting moment. Figure 4 shows the variation relationships of time and sliding resistance, and the maximum resistance Fmax is the breakaway resistance.

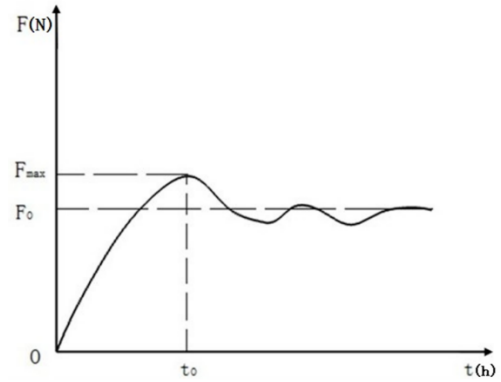

Figure 4. Variation relationships of time and sliding resistance

Adhesion occurring at the bottom of the vehicle occupies the max proportion of the breakaway resistance, it will reach 60%~75% of the breakaway resistance [23].

Soil Moisture Content

Influence effect to physical and mechanical properties of soil by moisture content is far above any other factors. There are four forms of soil water based on the quantity of water between the soil particles: 1) moisture content is less than plastic limit; 2) moisture content approach plastic limit; 3) moisture content approach liquid limit; 4) moisture content is over liquid limit. The moisture level of the deep soft terrain investigated here exceeds the liquid limit. The soil particles are submerged in water and there is free water on the soil surface [17].

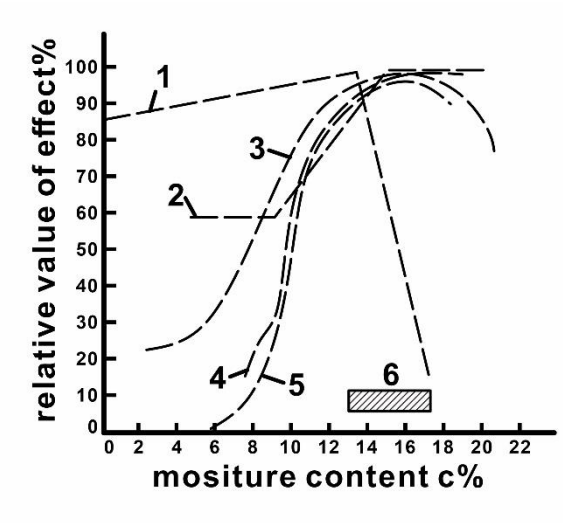

1: Shear resistance 2: Adhesive force 3: Compression

4: Ploughing resistance 5: Adhesion

6: Plastic deformation range

Figure 5. Influence rules of water on different mechanical properties of the soil

The influence rules of water on diverse mechanical properties of soil are different, the relation can be described as Figure 5. The activity of the soil particles and organic matter are intrinsic cause and the change of moisture content is the external reason.

Resistance-reduction by Air Curtain

The floating device is in adhesion friction state when there is sliding contacts between floating device and the deep soft clay. In this circumstance, there is a thin water film in some area between the floating device and soil. Surface tension of the water film, which determined by the factors about the thickness and continuity of the water film, will produce the adhesion. Contact area of water film will decrease while increasing the thickness of the water film or destroying the continuity of the water film, and the adhesion resistance of the floating device will be decreased.

The mechanism of sliding resistance reduction by air curtain for machine-soil coupled system has been discussed by Zhuge Zhen. There will be a series of circular air bubble spited out from the air vents under the bottom when the machine model moving on the deep soft clay. Therefore, on a certain level, the air bubble under the machine model can be assumed as a layer of air curtain.

The airflow with a certain pressure filled into the gap between floating device and soil. The airflow flows in the opposite direction to the sliding direction, and forms a thin air curtain. The air curtain will extend to the end of the floating device and the area of curtain is A1, as shown in Figure 6. The following prerequisites such as high soil surface density, medium soil moisture content and the proper thickness section of water film must be met for forming an idea air curtain layer.

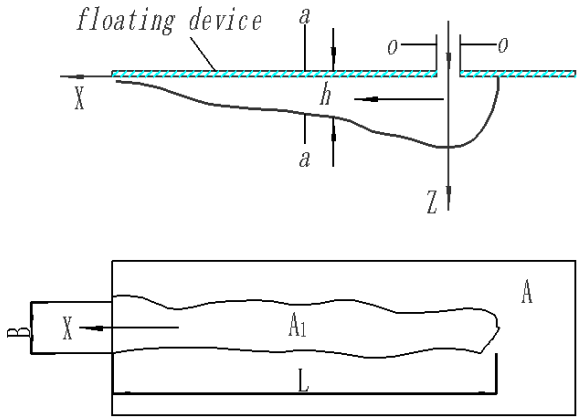

Figure 6. Jet air into the gap between the floating device and soil

Saturated soil of silty clay has been selected as research object and the model of interaction between the bottom of the floating device and airflow has been established. The sliding resistance of floating device can be analyzed into two parts as follows.

(1) Frictional resistance F1 between the floating device and air curtain. Supposing the length of the air space layer represents L and the average width represents B. The air space layer area A1= BL. The width is variant in the direction of length. The variant is random depending on the stochastic factors such as soil irregularities and evenness extent of ground bearing distribution of floating device. Therefore, supposing that the width is invariant in the direction of length and taking average value as the width of air space layer, the frictional resistance F1 can be expressed as follow:

$$F_1 = \int_0^L \tau_1 B dx \tag{2}$$

Where τ1(Pa·s) is tangential frictional resistance between the floating device and air curtain.

(2) Adhesion frictional resistance F2 between the floating device and soil beyond the air curtain. Assuming the total vertical pressure of floating device by air curtain is P1, F2 can be expressed as formula (3).

$$F_2 = (A - A_1)c + (P - P_1)\tan\varphi \tag{3}$$

Based on above analyses, the total sliding resistance can be expressed as formula (4).

$$F = F_1 + F_2 \tag{4}$$

The airflow of air curtain is composed of shear flow caused by floating device sliding and pressure flow formed by air source inflating. The effect of shear flow could be neglected and consider only the pressure flow due to that the sliding velocity is far less than average speed (10m/s) of pressure flow. Because of the thickness of the air curtain is very less than the width and the air flow is slit flow and it has the feature of laminar flow, the shear stress of pressure flow as laminar flow can be calculated as τ1 in formula (2). Obviously, frictional resistance F1 between the floating device and air curtain will much less than fictional resistance F2 between the floating device and soil beyond the air curtain. Thus, the frictional resistance F1 is neglected when calculating the resistance of the floating device under the air curtain condition, shown as formula (5):

$$F \approx F_2 = (A - A_1)c + (P - P_1)\tan\varphi \tag{5}$$

The parameter of resistance reduction rate η has been introduced, shown as formula (6):

$$\eta = \frac{F_0 - F}{F_0} \tag{6}$$

The air curtain area A1 will decrease the adhesion resistance between the floating device and soil according to the analyses above. The resistance and the rate of resistance reduction under the condition of air inflation are associated with the characteristics of the air curtain, like its pressure, thickness, and average width. These features are influenced by some factors such as the flow rate and the pressure of the air curtain.

EXPERIMENTAL PRINCIPLE AND OPERATING METHOD

Experimental equipment

Table 1 presents the experiment equipment parameters. The sliding resistance can be obtained in real-time by the force sensor placed on the front of the traction frame. The soil bin testing equipment is shown in Figure 7.

Table 1. Parameters of experiment equipment

Parameter	Value
Overall size of the soil bin (length×width×height)	46m×2m×1m
Overall size of the trolley (length×width×height)	2.5 m×2.4m×1.8m
Total mass of the trolley	1000kg
Power of the pulling-motor	55kw
Pulling speed of the trolley	0.3km/h~10km/h

Figure 7. Soil bin experiment equipment

Scala Model in Experiments

Suitable scale model will result in reducing the negative influence on test efficiency, which is caused by the dimension of the experimental subject. Typically, when building the scale model, the length reduction scale Cl is considered first. Since Cl functions as the basis for transforming other physical parameters. In the context of the vehicle-soil model, the scale model differs from the prototype model because of the soil stratification. The larger Cl, the greater the error will be. However, if Cl is overly small, the scale model will lose its original significance. Assume that the normal loading area is S (with the length l and width b) on floating device. The vehicle has a mass of 1200 kg, a length of 3600 mm, and a width of 1800 mm. According to the similarity theory, Cl has been determined to be 3. The scale model in the vehicle-soil system is presented as (7).

$$\begin{cases} C_A = C_l^2 \\ C_m = C_l^3 \\ C_p = C_l \\ C_v = C_l^{0.5} \end{cases} \tag{7}$$

Where CA represents the scale of area, Cm represents the scale of mass, CP represents the scale of ground pressure, and Cv represents the scale of velocity.

Equipment of Resistance Reduction by Air Curtain

With the similarity theory, the experiments of resistance reduction by air curtain have been designed via the soil bin experimental model, as shown in Figure 8. Three types of air curtain sprayer with a certain number of air vents have been designed. The diameter of air vents is 0.5mm, 1.0mm and 2.0mm respectively and each sprayer have the same total areas of air vents. Figure 9 shows the basic structure and working principle of air curtain generator.

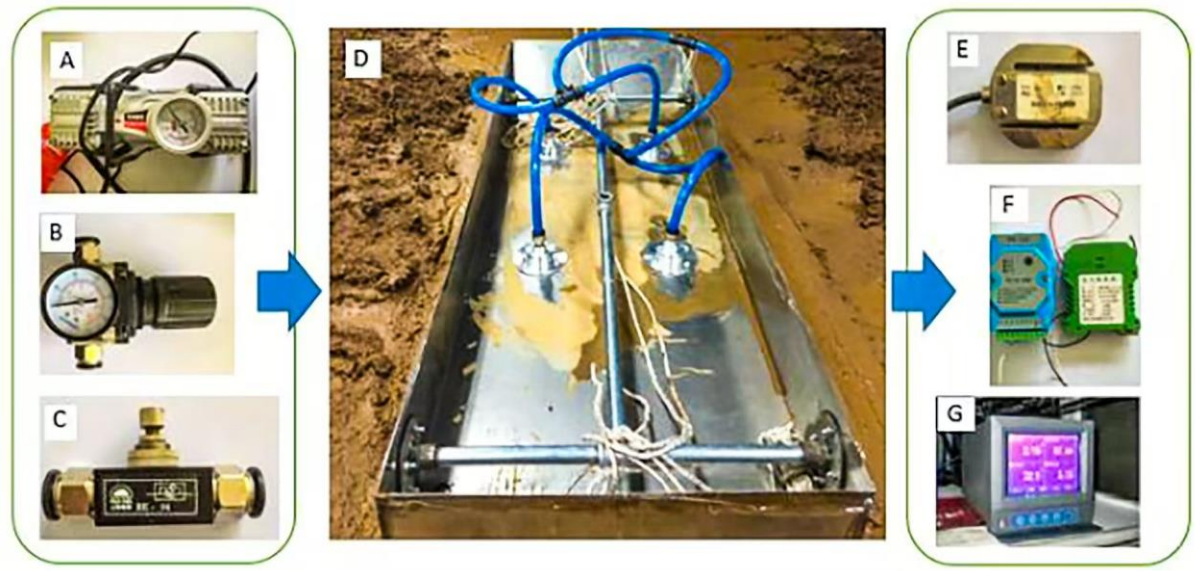

A: constant-flow pump; B: pressure regulating valve; C: throttle valve; D: floating device with air vents;

E: force sensor; F: signal spacers; G: data processing terminal

Figure 8. Experimental device of resistance reduction by air curtain

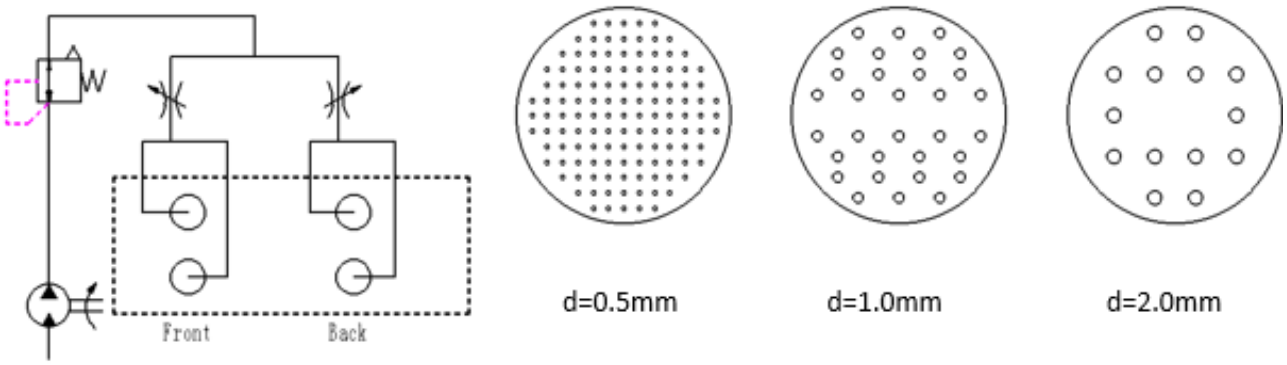

Figure 9. The principle of air curtain sprayer

Table 2. Parameters of air curtain sprayer

Parameter	Value
Maximum-flow of constant-flow pump	60*L/min*
Adjustable range of the pressure regulating valve	0~10kg/cm^2
Output signal range of the signal spacers	0~5*V*
Precision of the signal spacers	0.2%*FS*
Measurement range of the force sensor	0~50*kg*
Precision of the force sensor	0.03%*FS*

An adjustable constant flow pump is employed to provide airflow. The airflow is transmitted through a pressure-regulating valve and a throttle valve to the air curtain sprayer, which is installed on the bottom of the floating device. Then an air curtain will be

formed between the bottom and the soil. The resistance data will be collected by the force sensor and signal spacers, and subsequently these data will be processed by the programming terminal. The experimental instruments are listed in Table 2.

Soil Condition

Water level in the soil is one of the impacts affecting orthogonal tests. The moisture level of soil ||| is higher than that of soil ||, and the moisture level of soil || is higher than that of soil |. Their moisture contents are above the liquid limit. The soil for experiments has been confected using the silty clay, as shown in Figure 10. To ensure the results are accurate, reliable and comparable, the experiments will be firstly processed by the order that finish the experiments in soil |, then the experiments in soil ||, and then experiments in soil |||. Note that the soil must be plowed and leveled before each series of experiments to ensure that the experimental results are not affected by soil compaction resulting from repeated experiments.

(a) Soil I **(b) Soil II** **(c) Soil III**

Figure 10. Three kinds of soil condition

ORTHOGONAL EXPERIMENTS AND RESULT ANALYSIS

The floating devices have been designed and the aspect parameters is 1200mmx600mm. The ground pressure is capable of being controlled by adjusting the balance weight mass. The level of ground pressure is 0.5Kpa, 0.6Kpa and 0.7Kpa respectively. The maximum sliding speed of the floating device will be 6 kilometers per hour, equivalent to 1.67 meters per second. Its sliding velocity have been set as 0.5m/s, 0.8m/s, and 1.0m/s based on the principle of scale model. Four air curtain sprayers which diameter of air vents d=0.5mm have installed at the floating device and the flow rate Q of air curtain set at 40/min. The influencing factors and levels of the orthogonal experiments is presented in Table 3.

Figure 11 shows the sliding resistance changing trend of each experiments. The experimental data illustrates that breakaway resistance is bigger than steady resistance. The sliding resistance have been decreased by the air curtain not only the breakaway resistance but also the steady driving resistance. Taking the peak point as the breakaway resistance and the mean value of the steady travelling as the steady resistance, the experimental results summarized as Table 4.

Table 3. Orthogonal experiments

Factors	Level I	Level II	Level III
A: $p(Kpa)$	0.5	0.6	0.7
B: $v(m/s)$	0.5	0.8	1.0
C: Soil	Soil I	Soil II	Soil III

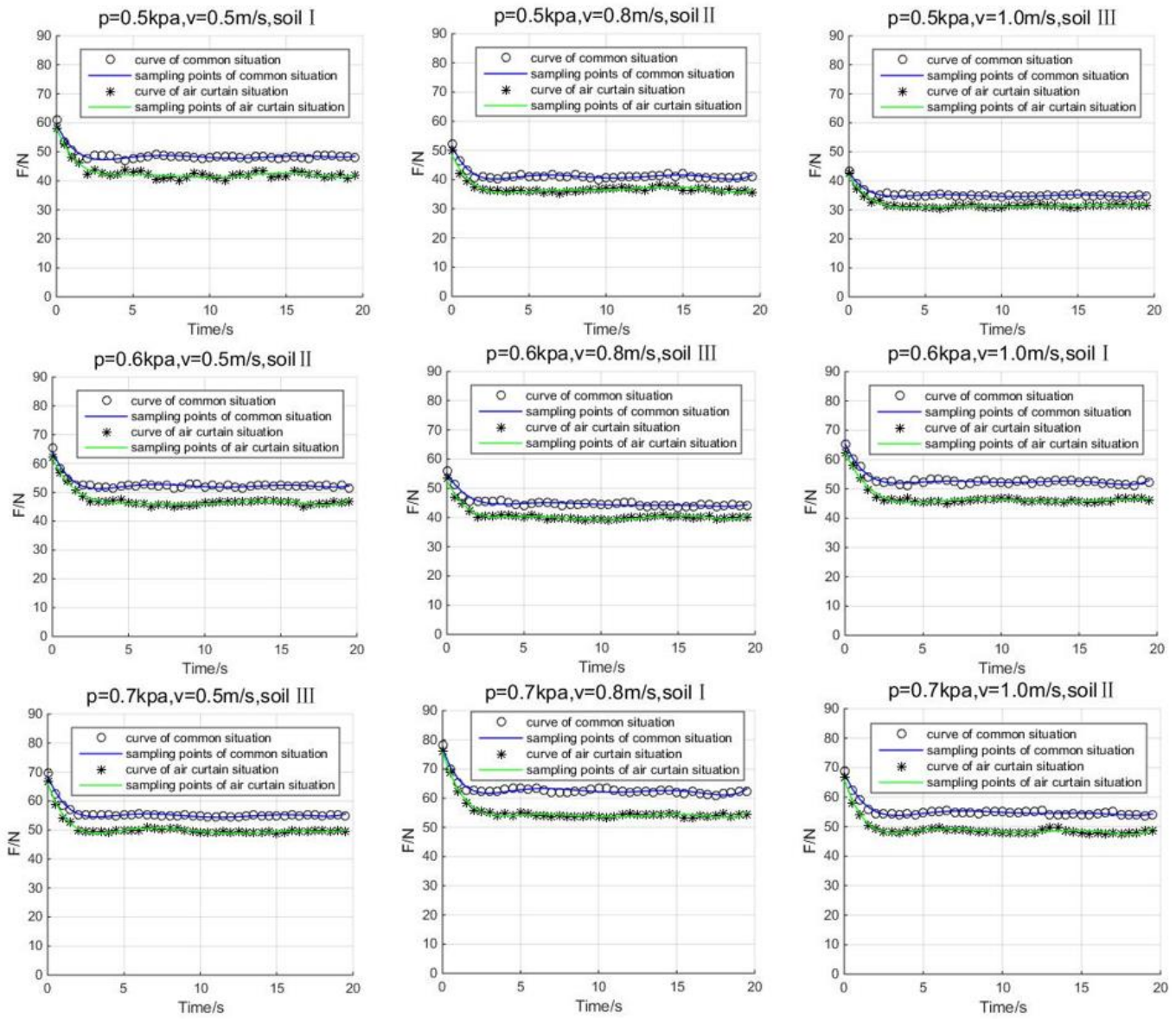

Figure 11. Curve of the resistance changing trend of orthogonal experiments

Tidying up and analyzing the data of table 4, it can be concluded that average breakaway resistance reduction rate is 3.91% and average steady resistance reduction rate is 11.17% by air curtain. Experimental results indicate that air curtain is effective for reducing the sliding resistance. Ground pressure is the most crucial factor for sliding resistance. The second most important one is soil moisture content, and the last one is the sliding velocity. The specific analysis is as follows:

(1) Ground pressure

The sliding resistance rises as the ground pressure increases, and the changing trend is independent of the air curtain. Meanwhile, the ground pressure has a minimal effect on the resistance reduction rate.

(2) Sliding speed

The greater the sliding speed, the larger the breakaway resistance. Meanwhile, the sliding speed has a negligible effect on the resistance reduction rate.

(3) Soil moisture content

In cases where the moisture content exceeds the liquid limit, the higher the moisture level, the smaller the sliding resistance. Also, the resistance reduction rate decreases as the moisture content increases.

Table 4. Orthogonal experiment results

Experiment number	$p(kpa)$	$v(m/s)$	Soil	Breakaway stage			Steady stage		
	A	B	C	Without air curtain	With air curtain	Resistance-reducing rate	Without air curtain	With air curtain	Resistance-reducing rate
1	1	1	1	60.9	58.08	4.63%	48.2	42.14	12.58%
2	1	2	2	52.2	49.89	4.41%	40.9	36.43	10.94%
3	1	3	3	43.5	42.61	2.03%	35.2	31.64	10.12%
4	2	1	2	65.3	60.07	4.94%	52.4	46.70	10.87%
5	2	2	3	56.1	53.35	4.90%	44.6	40.19	9.89%
6	2	3	1	65.2	62.17	4.65%	52.6	46.08	12.40%
7	3	1	3	69.6	66.96	3.79%	55.1	49.56	10.05%
8	3	2	1	78.3	75.94	3.01%	62.2	54.25	12.64%
9	3	3	2	68.7	66.78	2.79%	54.5	48.45	11.10%

SUPPORT VECTOR REGRESSION

Given the different driving conditions on deep soft terrain for the SFV, a support vector regression is incorporated to approximate and forecast the correlation between the influencing factors and the sliding resistance [24, 25]. This model has the ability to identify the position of the optimal separating hyperplane [26, 27]. In contrast to traditional machine learning algorithms, the support vector machine (SVM) is more suitable for scenarios where the number of samples is restricted [6].

The regression function is derived as follows:

$$f(\boldsymbol{x}) = w^{*}\Phi(\boldsymbol{x}) + b^{*} \tag{8}$$

where f(x) represents the predicted value, Φ(x) represents a non-linearity function.

According to [6], the weight vector w* and the bias b* are established by

$$w^{*} = \sum_{i=1}^{l}(\alpha_i - \alpha_i^{*})\Phi(\boldsymbol{x}_i) \tag{9}$$

$$\begin{cases} b^{*} = \frac{1}{N_{nsv}}\{G_1 + G_2\} \\ G_1 = \sum_{0<\alpha_i<C}[y_i - \sum_{x_i \in SV}(\alpha_i - \alpha_i^{*})K(\boldsymbol{x}_i, \boldsymbol{x}_j) - \varepsilon] \\ G_2 = \sum_{0<\alpha_i<C}[y_j - \sum_{x_j \in SV}(\alpha_j - \alpha_j^{*})K(\boldsymbol{x}_i, \boldsymbol{x}_j) - \varepsilon] \end{cases} \tag{10}$$

where xi represents the support vector, Nnsv represents the number of support vectors, $K(\boldsymbol{x}_i, \boldsymbol{x}_j) = \Phi(\boldsymbol{x}_i)\Phi(\boldsymbol{x}_j)$ represents the kernel function, y represents the real value, and $(\alpha_i - \alpha_i^{*})$ is non-zero. The ε-insensitive loss function can be described as

$$L(f(\boldsymbol{x}), y, \varepsilon) = \begin{cases} 0 & , |y - f(\boldsymbol{x})| \leqslant \varepsilon \\ |y - f(\boldsymbol{x})| - \varepsilon & , |y - f(\boldsymbol{x})| > \varepsilon \end{cases} \tag{11}$$

$$\begin{cases} max\{T_1 + T_2\} \\ T_1 = -\frac{1}{2}\sum_{i=1}^{l}\sum_{j=1}^{l}(\alpha_i - \alpha_i^{*})(\alpha_j - \alpha_j^{*})K(\boldsymbol{x}_i, \boldsymbol{x}_j) \\ T_2 = -\sum_{i=1}^{l}(\alpha_i + \alpha_i^{*})\varepsilon + \sum_{i=1}^{l}(\alpha_i - \alpha_i^{*})y_i \\ s.t. \begin{cases} \sum_{i=1}^{l}(\alpha_i - \alpha_i^{*}) \\ 0 \leqslant \alpha_i \leqslant C\ , 0 \leqslant \alpha_i^{*} \leqslant C \end{cases} \end{cases} \tag{12}$$

where C represents the penalty factor.

Note that the optimal solutions to the equation are $\alpha = [\alpha_1, \alpha_2, \ldots, \alpha_l]$and $\alpha^{*} = [\alpha_1^{*}, \alpha_2^{*}, \ldots, \alpha_l^{*}]$.

Thus,

$$f(\boldsymbol{x}) = \sum_{i=1}^{l}(\alpha_i - \alpha_i^{*})\Phi(\boldsymbol{x}_i)\Phi(\boldsymbol{x}) + b^{*} = \sum_{i=1}^{l}(\alpha_i - \alpha_i^{*})K(\boldsymbol{x}_i, \boldsymbol{x}) + b^{*} \tag{13}$$

According to the Eqs. (8) -(13), the SVR model is established. Forty random samples are adopted as the train set from experimental data presented in Table 5, while the other samples make up the test set, which can assess the model. Initially, normalization procedure is performed on the experimental data. The radial basis function is chosen as the kernel function. Once the training is finished, the SVR model can be utilized for simulation and prediction. Afterwards, the predicted values are compared with the experimental results, which is illustrated in Table 6.

Table 5. Sliding resistance at stable stage on soil III.

$Q(L/min)$	$v(m/s)$	Sliding resistance (N) for the following P(KPa)					
		0.4	0.5	0.6	0.7	0.8	0.9
20	0.5	16.82	29.14	42.32	54.21	67.14	79.93
	0.8	20.45	32.21	45.63	50.93	70.45	83.47
	1.0	23.35	35.83	47.27	52.54	72.83	85.56
40	0.5	12.44	24.36	37.06	49.64	62.46	74.92
	0.8	16.65	28.74	40.25	53.43	65.23	77.38
	1.0	20.94	31.64	43.12	56.67	67.02	79.13
60	0.5	10.77	24.65	33.32	46.87	58.98	70.25
	0.8	15.34	27.23	37.51	49.24	61.84	73.02
	1.0	17.52	29.26	40.91	52.98	63.43	75.51

Based on the result comparison, the mean square errors of the train set and test set are 0.5254 and 0.6057 respectively. Also, the determination coefficients R2 of the train set and test set are 0.9745 and 0.9676 respectively. Regarding sliding resistance, the experimental results indicate that the prediction model exhibits a favorable prediction ability with a limited number of samples.

Table 6. Contrast of the experimental data at a velocity of 1.0 m/s with SVR model.

$Q(L/min)$		Sliding resistance (N) for the following P (KPa)					
		0.4	0.5	0.6	0.7	0.8	0.9
20	Experiments	23.35	35.83	47.27	52.54	72.83	85.56
	SVR model	24.43	36.35	48.02	54.64	74.52	86.73
40	Experiments	20.94	31.64	43.12	56.67	67.02	79.13
	SVR model	21.76	31.17	43.26	56.26	67.73	80.48
60	Experiments	17.52	29.26	40.91	52.98	63.43	75.51
	SVR model	18.33	30.17	41.88	53.63	64.61	75.97

CONCLUSION

The characteristics of sliding resistance on the floating device of an A-ATV when sliding on deep soft terrain were discussed. The mechanism of reducing adhesion resistance by air curtain was analyzed on the soil with high moisture content. Corresponding experimental equipment was established using the soil bin experimental model. The SVR model for predicting the sliding resistance was introduced. The study results are as follows:

(1) Orthogonal experiments have proved that it is feasible to use air curtain to reduce the sliding resistance. The sliding resistance of the floating device with air curtain is lower than that of the floating device without air curtain.

(2) In the driving environment of clay with high moisture content, the sliding resistance reduces as the moisture level of the clay increases. If the moisture level exceeds the liquid limit, the resistance reduction rate decreases with the increasing moisture level, and the tendency is more pronounced in steady travelling. It indicates that, under the same environmental parameters, the steady resistance reduction rate is greater than the breakaway resistance reduction rate.

(3) The prediction tendency made by the SVR model is consistent with the experiment results. This demonstrates that the approach is able to obtain the optimum solution with a limited number of samples. Consequently, the SVR model is highly useful for fitting and predicting the correlations among the resistance, the sliding velocity, the pressure, and the flow of air curtain.

The research in this paper can help researchers to make sense of the sliding resistance and to investigate the drag reduction method for SFVs travelling on deep soft terrains. Moreover, the actual environment of deep soft terrains is complex and varied. When the sliding resistance is constrained by external factors in deep soft terrains, the active resistance reduction by air curtain method still can be used to improve the resistance of SFVs. It enhances the operational efficiency of floating-submerging vehicles, thereby having important engineering application value.

However, due to the absence of essential experimental conditions and apparatus, the sliding resistance of the SFV is merely investigated within the identical soil with varying moisture contents. In future work, a research on the resistance sliding situations in different deep soft soil conditions will be carried out.

ACKNOWLEDGMENT

This work was done with support from the Key Technologies Research and Development Program (grant no. 2022YFG2001303-2), and the Science and Technology Major Project of Guangxi (grant no. AB22035021).

REFERENCES

[1] X. Xie, F. Gao, C. Huang, et al. "Design and development of a new transformable wheel used in amphibious all-terrain vehicles (A-ATV)." Journal of Terramechanics, 2017, 69: 45-61.

[2] Y. Wang, Z. He, and J. Wang. "Effects of boat-type parameters of boat-type tractor on working resistance and subsidence depth. " Journal of Zhejiang University (Agriculture and Life Sciences), 2020, 46(6): 759-766. (in Chinese with English abstract)

[3] X. Yao, G. Xu, and Y. Cui. "Variable-diameter mobile platform chassis characteristics analysis." In 2011 International Conference on New Technology of Agricultural, IEEE, 2011: 166-169.

[4] J. Liu, F. Gao, G. Xu, et al. "Review and developing tendency of sliding unconventional walking." Journal of Mechanical Engineering, 2012, 48(24): 73-86. (in Chinese with English abstract)

[5] J. Liu, F. Gao, and G. Xu. "The research of sliding boot design based on compliance characteristic." Applied Mechanics and Materials, 2013, 365: 498-504.

[6] [6]C. Huang, F. Gao, X. Xie, et al. "The sinkage characteristics and the supporting capacity of a submerged floating vehicle driving in deep soft terrains. "Proceedings of the Institution of Mechanical Engineers, Part D: Journal of Automobile Engineering, 2018, 232(6): 725-737.

[7] L. Q. Ren, J. Tong, J. Q. Li, et al. "Soil adhesion and biomimetics of soil-engaging components: a review." Journal of Agricultural Engineering Research, 2001,79 (3): 239-264.

[8] M. Ahmadzadehtalatapeh, and M. Mousavi. "A review on the drag reduction methods of the ship hulls for improving the hydrodynamic performance." International Journal of Maritime Technology, 2015, 4: 51-64.

[9] X. Zhao and Z. Zhi, "Experimental and numerical studies on the air-injection drag reduction of the ship model." Ocean Engineering, 2022, 251: 111032.

[10] K. Xu, X. Su, R. Bensow, et al. "Drag reduction of ship airflow using steady Coanda effect." Ocean Engineering, 2022, 266: 113051.

[11] H. An, H. Pan, and P. Yang. "Research Progress of Air Lubrication Drag Reduction Technology for Ships." Fluids, 2022, 7 (10): 319.

[12] J. Zhang, S. Yang, and J. Liu. "Numerical investigation of frictional drag reduction with an air layer concept on the hull of a ship." Journal of Hydrodynamics, 2020, 32(3): 591-604.

[13] X. Zhao and Z. Zong. "Experimental and numerical studies on the air-injection drag reduction of the ship model." Ocean Engineering, 2022, 251: 111032.

[14] T. Tanaka, Y. Oishi, H. J. Park, et al. "Frictional drag reduction caused by bubble injection in a turbulent boundary layer beneath a 36-m-long flat-bottom model ship." Ocean Engineering, 2022, 252: 111224.

[15] M. E. McCormick and R. Bhattacharya. "Drag reduction of a submersible hull by electrolysis. " Naval Engineers Journal, 1973, 85(2): 11-16.

[16] N. K. Madavan, C. L. Merkle and S. Dentsch. "Numerical investigations mechanisms of microbubble drag reduction. " Journal of Fluids Engineering, 1985, 107: 370-377.

[17] Z. Zhuge, L. Wang, Q. Zhuge, et al. "Inquiry into mechanism of reduction of metal-soil resistance by air curtain." Journal of Wuhan Institute of Technology, 1992, 14(2): 27-32. (in Chinese with English abstract)

[18] C. W. Cheah, M. N. A. Karim, and Y. S. Lee. "The Accuracy and Error of Ground Penetrating Radar System with Machine Learning Support Vector Regression Technique." Journal of Advanced Research in Applied Sciences and Engineering Technology, 2025, 50: 191-202.

[19] M. El-Rawy, M. K. Abd-Ellah, H. Fathi, et al. "Forecasting effluent and performance of wastewater treatment plant using different machine learning techniques. " Journal of Water Process Engineering, 2021, 44:102380.

[20] D. Shakya, V. Deshpande, M. Agarwal, et al. "Standalone and ensemble-based machine learning techniques for particle Froude number prediction in a sewer system. " Neural Computing and Applications, 2022, 34(18), 15481–15497.

[21] J. Latif, C. Xiao, A. Imran, et al. "Medical imaging using machine learning and deep learning algorithms: a review." In 2019 2nd International conference on computing, mathematics and engineering technologies (iCoMET), pp. 1-5. IEEE, 2019.

[22] N. H. Tandel, H. B. Prajapati, and V. K. Dabhi. "Voice recognition and voice comparison using machine learning techniques: A survey." In 2020 6th International Conference on Advanced Computing and Communication Systems (ICACCS), IEEE, 2020: 459-465.

[23] J. Y. Wong. "Theory of ground vehicles. ", John Wiley & Sons, 2022.

[24] O. A. Montesinos López, A. Montesinos López, and J. Crossa. "Support vector machines and support vector regression." In Multivariate Statistical Machine Learning Methods for Genomic Prediction, Cham: Springer International Publishing, 2022: 337-378.

[25] V. Cherkassky and Y. Ma, "Practical selection of SVM parameters and noise estimation for SVM regression. " Neural Networks, 2004, 17(1): 113–126.

[26] S. Huang, N. Cai, P. P. Pacheco, et al. "Applications of support vector machine (SVM) learning in cancer genomics." Cancer genomics & proteomics, 2018, 15 (1): 41-51.

[27] S. Hosseinzadeh and M. Shaghaghi. "GPR data regression and clustering by the fuzzy support vector machine and regression." Progress In Electromagnetics Research M, 2020, 93: 175-184.